

Genetic analysis of D-xylose metabolism pathways in *Gluconobacter oxydans* 621H

Minhua Zhang · Liuqing Wei · Yi Zhou ·
Liqin Du · Tadayuki Imanaka · Qiang Hua

Received: 4 December 2012 / Accepted: 17 January 2013 / Published online: 5 February 2013
© Society for Industrial Microbiology and Biotechnology 2013

Abstract D-xylose is one of the most abundant carbohydrates in nature. This work focuses on xylose metabolism of *Gluconobacter oxydans* as revealed by a few studies conducted to understand xylose utilization by this strain. Interestingly, the *G. oxydans* 621H $\Delta mgdh$ strain (deficient in membrane-bound glucose dehydrogenase) was greatly inhibited when grown on xylose and no xylonate accumulation was observed in the medium. These experimental observations suggested that the *mgdh* gene was responsible for the conversion of xylose to xylonate in *G. oxydans*, which was also verified by whole-cell biotransformation. Since 621H $\Delta mgdh$ could still grow on xylose in a very small way, two seemingly important genes in the oxo-reductive pathway for xylose metabolism, a xylitol dehydrogenase-encoding *gox0865* (*xdh*) gene and a putative xylulose kinase-encoding *gox2214* (*xk*) gene, were knocked out to investigate the effects of both genes on xylose metabolism. The results showed that the *gox2214* gene was not involved in xylose metabolism, and there might be other genes encoding xylulose kinase. Though the *gox0865* gene played a less important role in xylose metabolism compared to the *mgdh* gene, it was significant in xylitol utilization in *G. oxydans*, which meant that *gox0865* was a necessary gene for the oxo-reductive pathway of xylose in vivo. To sum up,

when xylose was used as the carbon source, the majority of xylose was directly oxidized to xylonate for further metabolism in *G. oxydans*, whereas only a minor part of xylose was metabolized by the oxo-reductive pathway.

Keywords *Gluconobacter oxydans* · Xylose metabolism · Membrane-bound glucose dehydrogenase · Xylitol dehydrogenase · Xylulose kinase

Introduction

D-xylose, abundant in lignocellulosic biomass, is one of the most abundant carbohydrates in the biosphere. There are four routes for D-xylose metabolism in microorganisms. (1) The isomerase pathway. In numerous bacteria including *Escherichia coli* [3], *Bacillus* species [14] and *Lactobacillus* species [6], xylose is converted by xylose isomerase and xylulose kinase to xylulose-5-phosphate as an intermediate, which is further utilized by the pentose phosphate pathway. (2) The oxo-reductive pathway. In most fungi [12], xylose is transformed into the same intermediate xylulose-5-phosphate via xylose reductase, xylitol dehydrogenase and xylulose kinase, and then turns to the pentose phosphate pathway, as well. (3) Weimberg pathway. In *Pseudomonas fragi* [20], *Caulobacter crescentus* [18] and Halophilic Archaeon *Haloferax volcanii* [13], xylose is converted to α -ketoglutarate, an intermediate of the tricarboxylic acid cycle, by xylose dehydrogenase, xylonolactonase and xylonate dehydratase. (4) Dahms pathway. The Dahms pathway starts with the Weimberg pathway, but 2-keto-3 deoxy-xylonate is split by an aldolase to pyruvate and glycolaldehyde [17].

Gluconobacter oxydans, one of the most widely used biocatalysts in bioindustry and the chiral synthetic field, is

Minhua Zhang and Liuqing Wei contributed equally to this work.

M. Zhang · L. Wei · Y. Zhou · T. Imanaka · Q. Hua (✉)
State Key Laboratory of Bioreactor Engineering,
East China University of Science and Technology,
Shanghai 200237, China
e-mail: qhua@ecust.edu.cn

L. Du
College of Life Science and Technology, Guangxi University,
100 Daxue Road, Nanning 530005, Guangxi, China

able to incompletely oxidize a wide range of carbohydrates and alcohols. Most of these reactions are catalyzed by many highly active dehydrogenases located on the cell membrane, which makes *G. oxydans* the ideal strain for industrial microbiological production. In contrast to several well-studied carbon sources for *G. oxydans*, such as sorbitol, mannitol, glycerol and glucose, the mechanism of xylose metabolism pathways in *G. oxydans* has rarely been studied, thus construction of a xylose metabolism pathway is of significance to completing the metabolism pathway of *G. oxydans*, and may be of help in figuring out a different pathway from those described above. Deppenmeier and Ehrenreich [4] proposed a pathway similar to the oxo-reductive pathway for xylose metabolism in *G. oxydans*, as some key genes in the oxo-reductive pathway could be found in the genome of *G. oxydans* (Fig. 1). Buchert and Viikari [2] experimentally demonstrated that most of xylose was converted to xylonate by xylose dehydrogenase for further oxidation, however little was known about the gene involved in xylose oxidation. This study, therefore, focuses on unveiling the predominant xylose metabolic pathways in *G. oxydans* by genetic analysis.

In this study, to achieve understanding of the mechanisms underlying xylose metabolism in *G. oxydans*, we observed that the growth profiles (growth rate, xylonate concentration and pH value in the culture broth) of the membrane-bound glucose dehydrogenase deficient strain 621H $\Delta mgdh$ (the *mgdh* gene deletion mutant, previously constructed in our lab [22]) on xylose were significantly different from those of the wild-type *G. oxydans*. Therefore, the role of the membrane-bound glucose dehydrogenase in xylose metabolism was investigated. In addition, two strains deficient in xylitol dehydrogenase (XDH) and

putative xylulose kinase (XK), respectively, were also constructed and the functions of both the *xdh* and the *xk* genes were investigated.

Materials and methods

Strains, plasmids, and culture conditions

The strains and plasmids used in this study are listed in Table 1. *G. oxydans* 621H was pre-incubated in yeast–sorbitol (Y–S) medium (yeast extract 20 g/L, sorbitol 80 g/L). To test its growth, different media including yeast–xylose (Y–X) medium (yeast extract 20 g/L, xylose 40 g/L) and yeast–xylitol (Y–XT) medium (yeast extract 20 g/L, xylitol 40 g/L) were used. All *G. oxydans* strains were cultivated at 30 °C, 220 rpm. *E. coli* strains were cultivated at 37 °C in Luria–Bertani medium (yeast extract 5 g/L, tryptone 10 g/L, NaCl 10 g/L) containing appropriate antibiotics.

Whole-cell biotransformation of xylose to xylonate by *G. oxydans*

The different *G. oxydans* cells cultivated in Y–S medium in late-exponential phase were harvested by centrifugation (12,000 rpm, 10 min, 4 °C), washed three times with physiological saline (0.9 % NaCl solution), and then resuspended in 0.1 M phosphate buffer (pH 6.0). Bioconversions were carried out in triplicate in 50 mL shake flasks, containing 3.0 g DCW/L cells and 20 g/L xylose at 220 rpm and 30 °C. Samples (1 mL) were taken at suitable intervals, and the supernatants were obtained after centrifuging at 12,000 rpm and 4 °C for 10 min.

General genetic techniques

Primers used in this study are listed in Table 2. DNA manipulation was in accordance with the standard protocols. For PCRs, genomic DNA isolated from *G. oxydans* 621H (DSM 2343) was used as a template. LATAq DNA polymerase (TaKaRa Biotechnol., Dalian, China) was used for PCR amplification in test reactions.

Construction of knockout plasmids

Plasmids used in this study are summarized in Table 1. To generate a gene replacement plasmid for the inactivation of the *xdh* gene, the strategy developed by Derbise [5] was employed. The upstream fragment *xdh1* and downstream fragment *xdh2* of the *xdh* gene in *G. oxydans* [16] as well as the kanamycin resistance gene (1.2 kb) from pET28 were amplified by PCR with primers listed in Table 2.

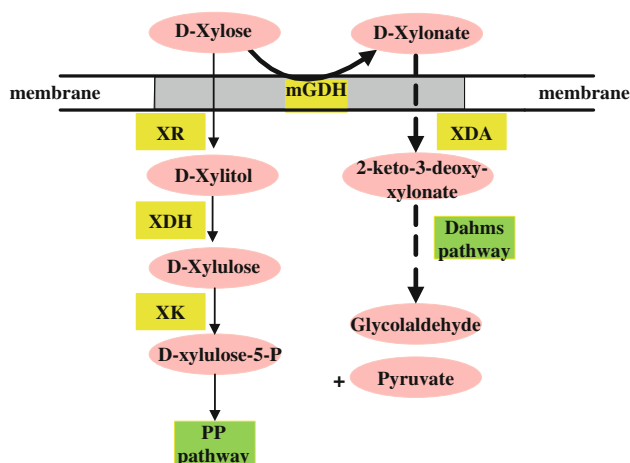


Fig. 1 Proposed scheme of xylose metabolism pathways in *G. oxydans*. XR, xylose reductase; XDH, xylitol dehydrogenase; XK, xylulose kinase; mGDH, membrane-bound glucose dehydrogenase; XDA, xylonate dehydratase. Definite reactions are indicated by solid arrows, predicted reactions are shown by broken arrows

Table 1 Strains and plasmids used in this study

Strains or plasmids	Relevant characteristics	Reference or source
Strains		
<i>G. oxydans</i> strains 621H (DSM2343)		Purchased from DSMZ
621H Δ <i>mgdh</i> (GDHK)	Gen ^f ; <i>G. oxydans</i> 621H derivative, <i>mgdh</i> ::Gen ^f	[22]
621H Δ <i>xdh</i>	Km ^r ; <i>G. oxydans</i> 621H derivative, <i>xdh</i> ::Km ^r	This study
621H Δ <i>xk</i>	Gen ^f ; <i>G. oxydans</i> 621H derivative, <i>xk</i> ::Gen ^f	This study
<i>E. coli</i> strains		
JM109	<i>recA1</i> , <i>endA1</i> , <i>gyrA96</i> , <i>thi</i> , <i>hsdR17</i> , <i>supE44</i> , <i>relA1</i> , Δ (<i>lac-proAB</i>)/F[<i>traD36</i> , <i>proab</i> ⁺ , <i>lacI</i> ^q , <i>lacZ</i> Δ M15]	
Plasmids		
pRK2013	Km ^r ; Helper plasmid for triparental mating;	ATCC
pSUP202	Amp ^r ; Tc ^r ; Cm ^r ; mob	
pSUP202 <i>xdh</i> ::Km	pSUP202 carrying <i>xdh</i> gene disrupted with Km ^r gene cassette	This study
pSUP202 <i>xk</i> ::Gen	pSUP202 carrying <i>xk</i> gene disrupted with Gen ^f gene cassette	This study

Table 2 Primers used in this study

Primer	Sequence(5'–3') ^a
<i>xdh1F-NcoI</i>	AATCCATGG GAACGGTATCGGAAATGCG
<i>xdh1R-KpnI-XbaI-EcoRI</i>	GGCGAATTC TCTAGA GGTACC CGGCATTGTTGAACAGGAAG
KmF- <i>KpnI</i>	GTAGGTACC ATAACCTCGTATAGCATAACATTATACGAAGTTATGCGAGGTATGTAGGCGG
KmR- <i>XbaI</i>	AATTCTAGAATAACTTCGTATAATGTATGCTATACGAAGTTATTTAGAAAAACTCATCGA
<i>xdh2F-XbaI</i>	AAGTCTAGA GCATCGTCAACACCGCCAGCAT
<i>xdh2R-EcoRI</i>	GGCGAATTC AAGTTCATCACCGCCAGA
<i>xdhF-EcoRI</i>	AAGGAATTC TCAAGGGGCTGCATGGGG
<i>xdhR-HindIII</i>	AATAAGCTT GCAAGATGGCTCGCAGGAC
<i>xk1F-NcoI-XbaI</i>	ATTCATGG TCTAGA TCGGTTGCGTTCAGGACG
<i>xk1R-MluI-KpnI-EcoRI</i>	ATTGAATTC GGTACC ACGCGT GTCCCGGAACACTTCATTG
GenF- <i>MluI</i>	CGGACGCGT CGTGGAAACGGATGAAGG
GenR- <i>KpnI</i>	ATC GGTACC TCTCGGCTTGAACGAATT
<i>xk2F-KpnI</i>	ATTGGTACC TCTGAAGCCCGACGAACA
<i>xk2R-EcoRI</i>	ACGGAATTC CCATTGCGGCATAGTTCAG
<i>xkF-EcoRI</i>	GCAGAATTC TCTGGAGGGTGTCAATGCG
<i>xkR-HindIII</i>	GCAAAGCTT CGTAGCGTTGTCAGGTATGG

^a Underlined sequences indicate restriction sites for restriction enzymes

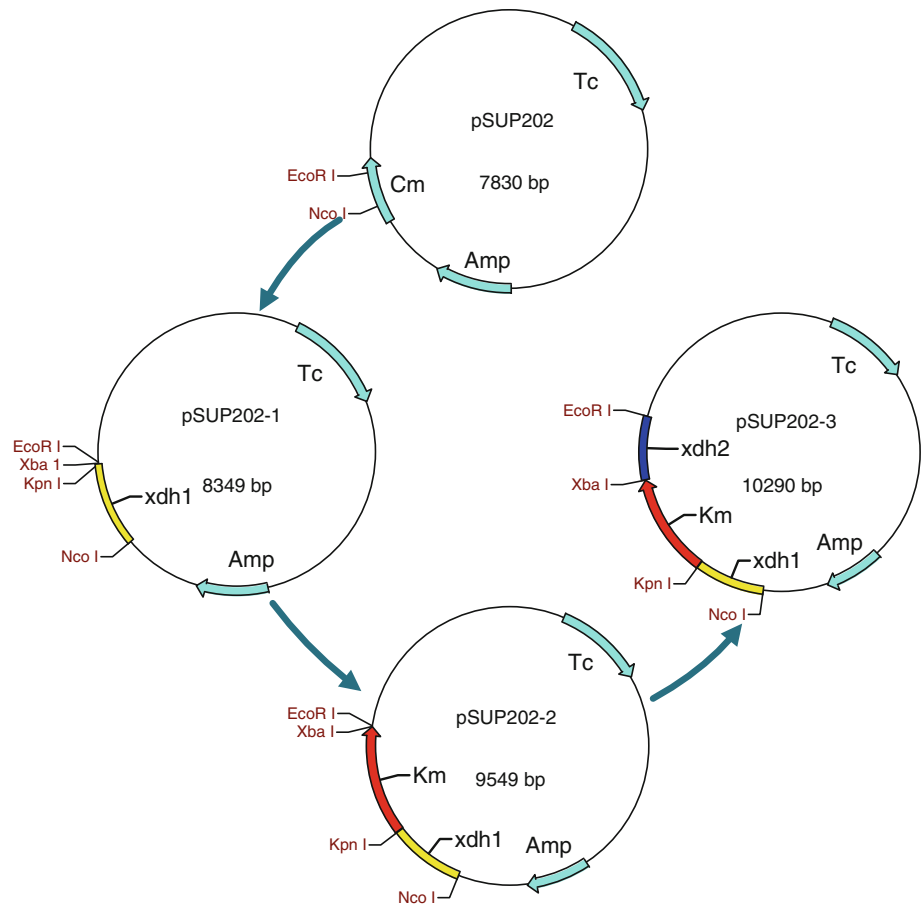
Construction steps of plasmid for disrupting the *xdh* gene are shown in Fig. 2. The strategy of plasmid construction for the inactivation of the *xk* gene was similar to that for the *xdh* gene except for the use of a gentamycin resistance cassette instead of a kanamycin resistance cassette.

Conjugational plasmid transfer into *G. oxydans*

Knockout plasmid pSUP202 *xdh*::Km or pSUP202 *xk*::Gen was transferred into *G. oxydans* by triparental mating, using *E. coli* JM109 harboring the knockout plasmid as the

donor strain and *E. coli* HB101 bearing vector pRK2013 as the helper strain. The strategy developed by Holscher and Gorisch [10] was adapted in this study. Three strains were grown to the late-exponential phase, pelleted, washed, resuspended in Y–S medium, and mixed at a 1:1:1 ratio. The mixture was spread on Y–S agar plates without antibiotics and incubated overnight at 30 °C. The grown cell patches were scraped from the plates and resuspended in sterile water, then streaked on selective Y–S agar plates containing appropriate selective antibiotic (gentamycin, kanamycin). Plates were incubated at 30 °C for 3–5 days

Fig. 2 Construction of knockout plasmid. The fragment *xdh1* containing part of the upstream *xdh* gene was amplified with primers *xdh1F-NcoI* and *xdh1R-KpnI-XbaI-EcoRI* and cloned between the *NcoI-EcoRI* sites of pSUP202, resulting in plasmid pSUP202-1. The fragment *Km* resistance gene was amplified with primers *KmF-KpnI* and *KmR-XbaI* and cloned between *KpnI* and *XbaI* of pSUP202-1, resulting in plasmid pSUP202-2. The fragment *xdh2* containing part of the downstream *xdh* gene was amplified with primers *xdh2F-XbaI* and *xdh2R-EcoRI* and cloned between the *XbaI-EcoRI* sites of pSUP202-2, resulting in plasmid pSUP202-3. The strategy for constructing the plasmid for the inactivation of the *xk* gene was the same as that for *xdh*, except that the resistance was replaced by gentamicin



until resistant colonies appeared. Extracting genomic DNA or plasmids of these resistant colonies, polymerase chain reaction, direct sequencing or restriction enzyme reaction were performed to remove false positives and to identify the objective mutations.

Enzyme activity assay

Xylitol dehydrogenase activity was measured spectrophotometrically at 30 °C by following the substrate-dependent formation of NADH at 340 nm [7]. The standard reaction mixture contained 100 mM Tris-HCl buffer (pH 9.5), 3 mM NAD⁺ and enzyme. The assay was started by addition of 100 mM xylitol.

Xylulose kinase activity was assayed by coupling the formation of ADP to the oxidation of NADH to NAD⁺ via pyruvate kinase and lactate dehydrogenase and monitored at 340 nm [9]. The standard reaction mixture contained 50 mM Tris buffer (pH 7.5), 10 mM MgSO₄, 1.2 mM ATP, 1.2 mM phosphoenolpyruvate, 0.3 mM NADH, 2 U of pyruvate kinase, 2 U of lactate dehydrogenase, and enzyme. The assay was started by addition of 1 mM D-xylulose.

The enzyme activity assays were carried out in triplicate. One enzyme unit was defined as the amount of the enzyme required to oxidize 1 μmol of substrate in 1 min. Total protein was determined by the Lowry method [11].

Detection of growth conditions

Strains were grown in 250 mL Erlenmeyer flasks containing 50 mL of Y-X or Y-XT medium. Cell growth was monitored by measuring the optical density at 600 nm. Dry cell weight (DCW) was determined by collecting cell pellets from 100 mL of culture aliquots, washing with distilled water, and drying at 100 °C until constant weight was reached. Xylose concentration was determined by xylose assay kit (Megazyme Intl, Wicklow, Ireland) with microplate spectrofluorometer (PowerWave XS/XS2, Bio-Tek Instruments, Winooski, VT) at 554 nm. Xylonate concentration was detected by high-pressure liquid chromatography (HPLC) on an Aminex HPX-87 Ion Exclusion column (Bio-Rad, Hercules, CA) with 5 mM sulfuric acid as a mobile phase. Every growth parameter was measured three times to get an accurate result.

Results

Growth profiles of *G. oxydans* 621H and 621H $\Delta mgdh$ in xylose medium

In our previous study [22], we constructed a 621H $\Delta mgdh$ strain that was deficient in membrane-bound glucose dehydrogenase (mGDH) to improve the growth rate and biomass yield of *G. oxydans* on glucose. Surprisingly, the growth of the 621H $\Delta mgdh$ mutant strain on xylose was significantly inhibited compared with that of the wild-type strain (final cell density dropped from 0.648 to 0.052 g DCW/L) (Fig. 3a). In addition, when the wild-type strain was cultured in a xylose medium, the xylonate concentration in the broth gradually accumulated to a final concentration of around 9.3 g/L and the pH value of the medium dropped rapidly after the lag phase, with a final pH value of 3.5 (Fig. 3b–d). All these cultural characteristics of the wild-type strain were similar to the observations by Buchert and Viikari [2]. The only difference was that pure xylose (without glucose addition) was used to cultivate *G. oxydans* 621H, in comparison to the yeast-xylose medium plus a little glucose used in the above literature.

In contrast, the maximum specific growth rate of the 621H $\Delta mgdh$ strain on xylose drastically decreased to below one-third of the wild-type strain (Table 3), and no obvious changes were found for the pH value and xylonate accumulation in the culture of the xylose-growing 621H

$\Delta mgdh$ strain. These results imply that xylonate might be an important carbon source for the growth of *G. oxydans*.

Whole-cell biotransformation of xylose to xylonate by different *G. oxydans*

In order to further ascertain whether the *mgdh* gene was the only gene involved in the bioconversion from xylose to xylonate of *G. oxydans*, the effects of xylose oxidation and xylonate formation by different whole-cell *G. oxydans* were also investigated. The different *G. oxydans* cells cultivated in Y–S medium in the late-exponential phase were harvested as whole-cell catalysts; after the *mgdh* gene was knocked out, no xylonate was produced, as shown in the HPLC graphics (Fig. 4), which implies that the bioconversion of xylose to xylonate was attributed to the *mgdh* gene. Therefore, in addition to the known function of oxidizing glucose, this study shows that the *mgdh* gene also works in the oxidization of xylose and thus plays an essential role in xylose metabolism in *G. oxydans*.

Confirmation of xylitol dehydrogenase and xylulose kinase deficient strains

Gluconobacter oxydans 621H $\Delta mgdh$ could still grow on xylose, albeit at a low growth rate, which indicates that there might be some other pathways for xylose metabolism in *G. oxydans*. It has been reported that xylose is mainly utilized by the oxo-reductive pathway in *G. oxydans*, and

Fig. 3 Growth profiles of *G. oxydans* 621H (square) and 621H $\Delta mgdh$ (triangle) in xylose medium. **a** Growth curves in Y–X medium; **b** pH value; **c** Xylose consumption and **d** Xylonate concentration

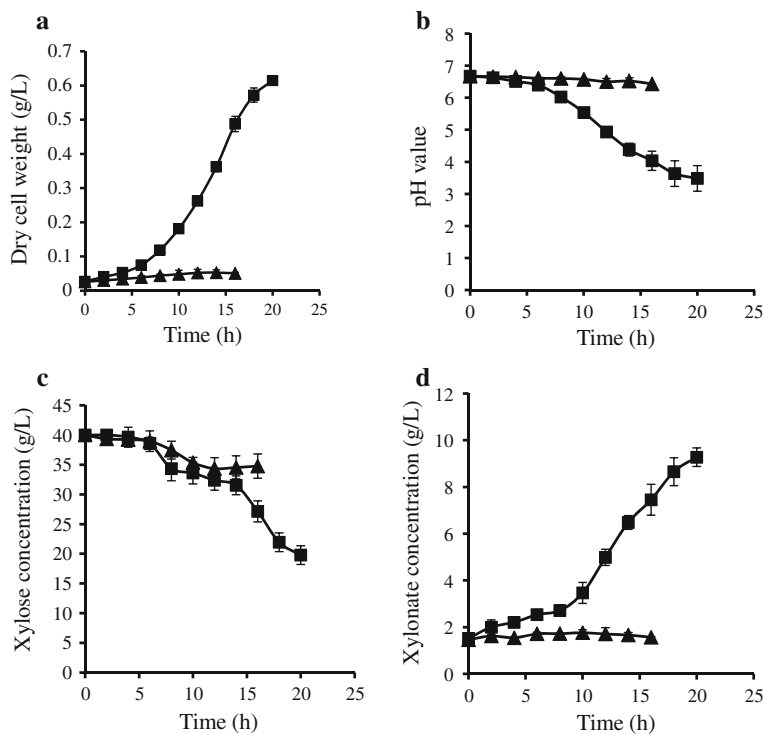


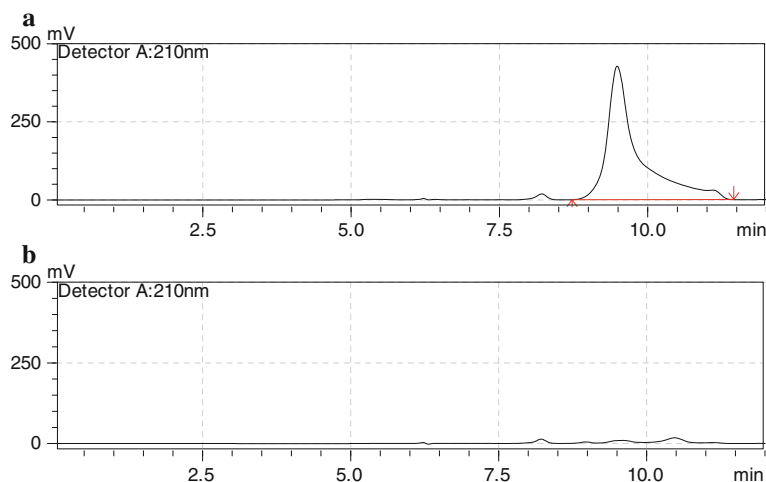
Table 3 Growth kinetic parameters for various *G. oxydans* strains with xylose or xylitol as the carbon source

Strain	40 g/L xylose		40 g/L xylitol	
	μ_{\max} (h ⁻¹) ^a	C_{\max} (gDCW/L) ^b	μ_{\max} (h ⁻¹)	C_{\max} (gDCW/L)
621H	0.231 ± 0.018	0.648 ± 0.007	0.259 ± 0.008	0.295 ± 0.002
621H Δxdh	0.193 ± 0.020	0.434 ± 0.017	0.139 ± 0.022	0.073 ± 0.001
621H Δxk	0.216 ± 0.012	0.639 ± 0.015	0.222 ± 0.002	0.266 ± 0.004
621H $\Delta mgdh$	0.067 ± 0.012	0.052 ± 0.003		

^a μ_{\max} maximum specific growth rate

^b C_{\max} maximum cell density

Fig. 4 HPLC graphics of biotransformation of xylose to xylonate by different whole-cell *G. oxydans*. **a** Xylonate production by *G. oxydans* 621H; **b** Xylonate production by 621H $\Delta mgdh$



most of the genes encoding enzymes of this pathway have already been identified from the genome sequence of *G. oxydans* [4]. Two key enzymes of this pathway, xylitol dehydrogenase and xylulose kinase, were studied here to confirm whether the oxo-reductive pathway is responsible for xylose metabolism.

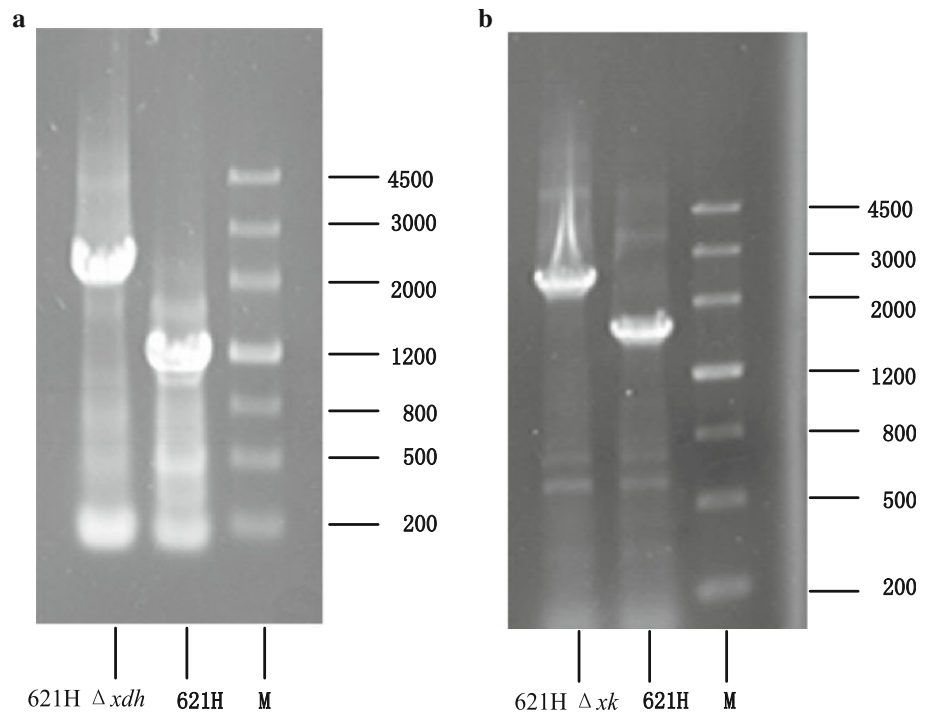
Xylitol dehydrogenase (EC 1.1.1.9) is one of the key enzymes of xylose utilization in yeast and fungi, which catalyses the reaction from xylitol to xylulose. In light of the genome sequence of *G. oxydans*, xylitol dehydrogenase is encoded by *gox0865*, whose characteristics have been fully investigated [19]. Xylulose kinase (EC 2.7.1.17) is another key enzyme for xylose utilization through the pentose phosphate (PP) pathway, which catalyses the conversion from xylulose to xylulose-5-P. Xylulose kinase has already been successfully isolated from bacteria, fungi and bovine liver. Pival et al. [15] have characterized D-xylulose kinase and recombinantly produced this protein in *E. coli* to improve the production of ethanol. Bu et al. [1] solubilized abundantly expressed xylulose kinase in *E. coli* by molecular chaperone GroEL-GroES. The *gox2214* gene in *G. oxydans* was annotated as a putative xylulose kinase. To provide biochemical evidence for the gene function, recombinant *G. oxydans* XK was successfully obtained

from *E. coli* by expressing it in a soluble form with chaperonins GroEL/GroES and purifying it using Ni-NTA affinity chromatography. Unfortunately, no xylulose kinase activity was detected for the purified enzyme (data not shown).

To confirm the function of the oxo-reductive pathway in xylose metabolism, mutant strains deficient in the *gox0865* gene (*xdh*, encoding xylitol dehydrogenase) or the *gox2214* gene (*xk*, encoding putative xylulose kinase) were constructed using a suicide vector pSUP202 harboring the *xdh* or *xk* gene, with an insertion of a kanamycin or gentamicin resistance cassette in the gene. The disruption was isolated as a strain with a phenotype of kanamycin and cephalosporine resistances (Km^rCep^r) or gentamicin and cephalosporine resistances (Gen^rCep^r) after conjugation transfer of the suicide plasmid pSUP202 *xdh*::Km or pSUP202 *xk*::Gen into *G. oxydans* 621H.

The disruption and absence of the wild type gene was confirmed by PCR. In Fig. 5, a lane sized about 2.4 kb was obtained from the 621H Δxdh strain due to the insertion of the Km resistance gene, and a lane sized about 2.3 kb was gained from the 621H Δxk strain due to the insertion of the Gen resistance gene, suggesting successful knockout of the *gox0865* or *gox2214* gene.

Fig. 5 PCR Confirmation of the disruption and absence of the *xdh* or *xk* gene. When *xdhF-EcoRI* and *xdhR-HindIII* were used as primers, a lane sized about 1.2 kb was obtained from the wild-type *G. oxydans* 621H strain, and a lane sized about 2.4 kb was obtained from the mutant 621H Δxdh strain due to the insertion of the Km resistance gene. When *xkF-EcoRI* and *xkR-HindIII* were used as primers, a lane sized about 1.6 kb was obtained from 621H, and a lane sized about 2.3 kb was obtained from the mutant 621H Δxk due to the insertion of the Gen resistance gene



Enzyme activity detection of xylitol dehydrogenase and xylulose kinase

To provide biochemical evidence of gene functions, enzyme activities of xylitol dehydrogenase and xylulose kinase were assayed for crude cell extracts of *G. oxydans* 621H mutants grown on xylose. In comparison to the wild-type strain, the xylitol dehydrogenase activity of 621H Δxdh mutant strain decreased by about 75 % (Fig. 6a), suggesting that most of the intracytoplasmic xylitol dehydrogenase was encoded by *gox0865*. The xylulose kinase activity, however, declined by only 30 % after deletion of the *xk* gene (Fig. 6b), implying that genes other than

gox2214 might be mainly responsible for the phosphorylation of xylulose in *G. oxydans*.

Culture of the wild-type and the mutant strains in xylose or xylitol medium

The growth performances of the two mutant strains and the wild-type strain in medium with xylose or xylitol as the carbon source were further investigated to validate the roles of both genes in xylose metabolism in *G. oxydans* (Fig. 7).

The wild-type strain could grow on xylose, which was quite different from previous reports stating that *G. oxydans* could not grow on pure xylose without the addition of a

Fig. 6 Enzyme activity detection of the xylitol dehydrogenase and the xylulose kinase

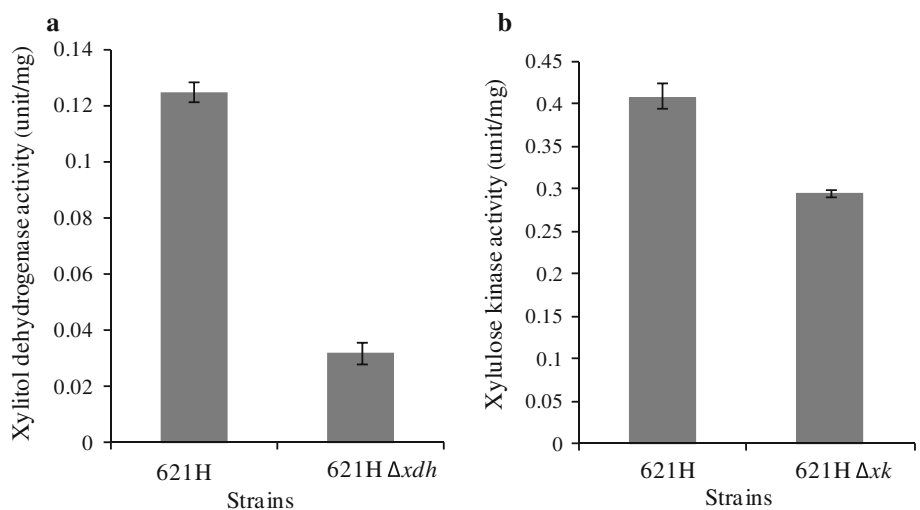
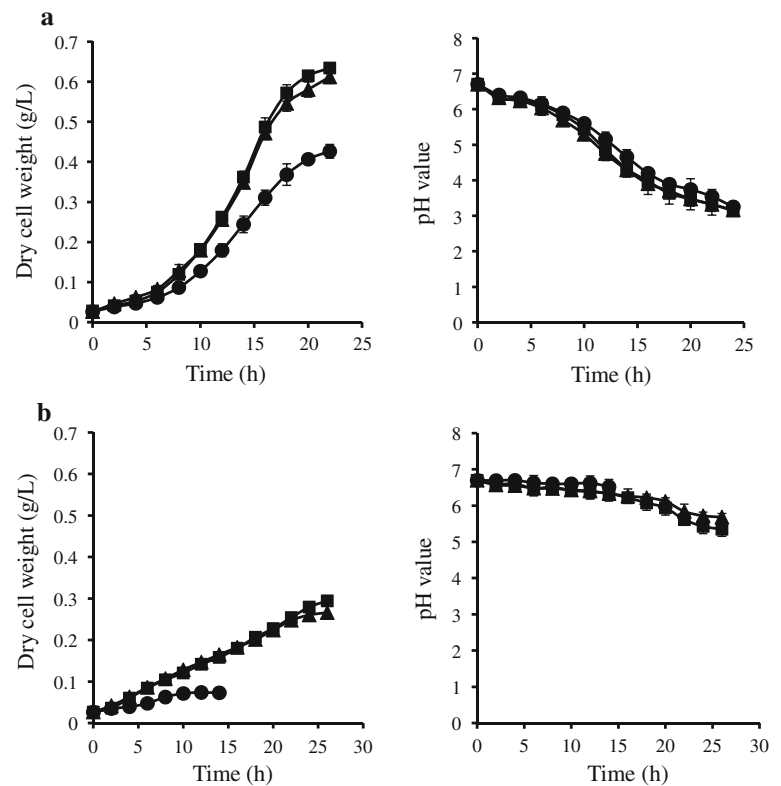


Fig. 7 Growth profiles of the wild-type *G. oxydans* 621H strain (*square*) and the mutant 621H Δxdh (*circle*) or 621H Δxk (*triangle*) strain in xylose or xylitol medium. **a** Growth profiles in xylose medium (Y–X medium); **b** Growth profiles in xylitol medium (Y–XT medium)



small amount of glucose [2]. When the wild-type strain was cultured in a xylose medium, the pH value of the medium started to drop significantly after the lag phase, and a final pH value of 3.5 and a maximum cell density of 0.648 gDCW/L were obtained. The extremely low pH value was caused by large amount of xylonate from the direct oxidation of xylose by membrane-bound glucose dehydrogenase. When xylitol, an intermediate of xylose metabolism, was used as the carbon source, the pH value of the medium decreased slowly and reached a final value of 5.4. The growth of the wild-type strain on xylitol, however, reduced by more than 50 % in DCW compared to that on xylose, implying the presence of other xylose metabolism pathways bypassing xylose, e.g. a xylonate metabolism pathway.

Whether grown on xylose or xylitol, the deficiency of *gox2214* gene caused only slight decreases in both maximum specific growth rate and maximum cell density in comparison to those of the wild-type *G. oxydans* (Fig. 7; Table 3). These experimental results, together with the finding that no xylulose kinase activity was detected for the purified enzyme, suggest that the *gox2214* gene might not be the major gene involved in xylose metabolism, and there might be other genes encoding xylulose kinase, which was in accordance with the enzyme activity detection results of both crude and pure enzymes of xylulose kinase.

Removal of xylitol dehydrogenase, however, resulted in more than 33 % (on xylose) and 72 % (on xylitol)

decreases in maximum cell density, and 16 % (on xylose) and 46 % (on xylitol) decreases in maximum specific growth rate (Table 3). These results suggest that the *xdh* gene investigated in this study was associated tightly with xylose utilization in *G. oxydans* through the oxo-reductive pathway. Moreover, the still fast growth of the 621H Δxdh strain on xylose, albeit slower than the wild-type strain, implies that there must be other pathways responsible for metabolizing the majority of xylose, which supported the above results. These observations suggest that since the *gox0865* gene played a relatively major role in the xylitol metabolism, *G. oxydans* 621H harbored at least one additional gene responsible for the utilization of xylitol.

In summary, based on the growth profiles of the 621H $\Delta mgdh$ strains, 621H Δxdh and 621H Δxk , it could be easily found that the majority of xylose was directly oxidized to xylonate for further metabolism in the cell. Only a small part of xylose was converted by xylitol dehydrogenase and xylulose kinase to obtain xylulose-5-phosphate for further assimilation via the PP pathway.

Discussion

In this study, we focused on the xylose metabolism of *G. oxydans*, which to date had received little study, by

analyzing the effects of the *mgdh*, *xdh* and *xk* genes on cell growth in either a xylose or a xylitol medium. Genetic disruption of *mgdh* was sufficient to completely abolish xylonate formation from xylose, which, however, severely inhibited the growth of *G. oxydans* on xylose (Fig. 7). The whole-cell biotransformation results also confirmed that the *mgdh* gene was the only gene related to the reaction from xylose to xylonate. The results imply that xylonate was the main carbon source utilized by *G. oxydans* in vivo. Meanwhile, the genetic and biochemical characterization of *xdh* showed it was responsible for the intercellular xylose metabolism process via oxo-reductive pathway. From all the experiments, it could be concluded that *G. oxydans* utilized xylose in two different ways: one was the direct oxidation of xylose into xylonate, which could then be transported through the cytoplasmic membrane for further metabolism; the other way included xylose uptake, intracellular oxidation and further dissimilation via the oxo-reductive pathway (Fig. 1). The former was identified as the major pathway of xylose utilization by *G. oxydans* during typical fermentation.

A question may arise as to how in vivo xylonate transported into the cytoplasm is metabolized in *G. oxydans*. At present, we know of the aforementioned four routes for D-xylose metabolism in microorganisms. Among these pathways, xylonate can be generated only by the Weimberg and Dahms pathways. Due to the absence of key enzymes of phosphofruktokinase and succinate dehydrogenase, the Embden-Meyerhof-Parnas (EMP) pathway and the tricarboxylic acid (TCA) cycle are not complete in *G. oxydans* [8]. The deficiency of the two key enzymes in the TCA cycle restrained the utilization of α -ketoglutarate, thus the Weimberg pathway [20] is not likely to contribute to the xylonate metabolism in *G. oxydans*. Hence, cytoplasmic xylonate can probably be utilized via the Dahms pathway [17] where pyruvate and glycolaldehyde will be generated to enter the central metabolism of *G. oxydans* (Fig. 1). An upcoming study will include the confirmation of the whole Dahms pathway and determination of xylose distributions between the oxo-reductive pathway and the Dahms pathway. Characterization of the key enzymes, such as D-xylonate dehydratase (catalyzing the conversion of D-xylonate to 3-deoxy-D-pentulosonic acid) and 3-deoxy-D-pentulosonic acid aldolase (splitting 3-deoxy-D-pentulosonic acid into pyruvate and glycolaldehyde) will be conducted to ascertain the existence of the Dahms pathway. In addition, metabolic stoichiometry and stable isotope-based flux analysis [21] are being developed to determine the contributions of individual pathways, which could therefore facilitate the engineering of *G. oxydans* for better growth and synthesis of useful enzymes on xylose from renewable hemicellulose biomass.

Acknowledgments This study was financially supported by the National Natural Science Foundation of China (No. 31200025), National Basic Research Program of China (973 Program) (2012CB721101), Natural Science Foundation of Shanghai (11ZR1408100), and partially supported by National Special Fund for State Key Laboratory of Bioreactor Engineering (2060204), Shanghai Leading Academic Discipline Project (B505) and the Fundamental Research Funds for the Central Universities.

References

- Bu S, Tsang PWK, Fu RZ (2005) GroEL-GroES solubilizes abundantly expressed xylulokinase in *Escherichia coli*. *J Appl Microbiol* 98(1):210–215
- Buchert J, Viikari L (1988) Oxidative D-xylose metabolism of *Gluconobacter oxydans*. *Appl Microbiol Biotechnol* 29(4): 375–379
- David JD, Wiesmeyer H (1970) Control of xylose metabolism in *Escherichia coli*. *Biochim Biophys Acta* 201(3):497
- Deppenmeier U, Ehrenreich A (2009) Physiology of acetic acid bacteria in light of the genome sequence of *Gluconobacter oxydans*. *J Mol Microbiol Biotechnol* 16(1–2):69–80
- Derbise A, Lesic B, Dacheux D, Ghigo JM, Carniel E (2003) A rapid and simple method for inactivating chromosomal genes in *Yersinia*. *FEMS Immunol Med Mic* 38(2):113–116
- Erlanson KA, Delamarre SC, Batt CA (2001) Genetic evidence for a defective xylan degradation pathway in *Lactococcus lactis*. *Appl Environ Microb* 67(4):1445–1452
- Girio FM, Pelica F, Amaral MT (1996) Characterization of xylitol dehydrogenase from *Debaryomyces hansenii*. *Appl Biochem Biotech* 56(1):79–87
- Greenfield S, Claus GW (1972) Nonfunctional tricarboxylic acid cycle and the mechanism of glutamate biosynthesis in *Acetobacter suboxydans*. *J Bacteriol* 112(3):1295–1301
- Gu Y, Ding Y, Ren C, Sun Z, Rodionov DA, Zhang WW, Yang S, Yang C, Jiang WH (2010) Reconstruction of xylose utilization pathway and regulons in Firmicutes. *BMC Genomics* 11(1):255
- Hölscher T, Görlich H (2006) Knockout and overexpression of pyrroloquinoline quinone biosynthetic genes in *Gluconobacter oxydans* 621H. *J Bacteriol* 188(21):7668–7676
- Hartree EF (1972) Determination of protein: a modification of the Lowry method that gives a linear photometric response. *Anal Biochem* 48(2):422–427
- Jeffries TW (2006) Engineering yeasts for xylose metabolism. *Curr Opin Biotech* 17(3):320–326
- Johnsen U, Dambeck M, Zaiss H, Fuhrer T, Soppa J, Sauer U, Schönheit P (2009) D-xylose degradation pathway in the halophilic archaeon *Haloferax volcanii*. *J Biol Chem* 284(40): 27290–27303
- Lindner C, Stülke J, Hecker M (1994) Regulation of xylanolytic enzymes in *Bacillus subtilis*. *Microbiol* 140(4):753–757
- Pival SL, Birner-Gruenberger R, Krump C, Nidetzky B (2011) D-xylulose kinase from *Saccharomyces cerevisiae*: isolation and characterization of the highly unstable enzyme, recombinantly produced in *Escherichia coli*. *Protein Expres Purif* 79(2):223–230
- Prust C, Hoffmeister M, Liesegang H, Wiezer A, Fricke WF, Ehrenreich A, Gottschalk G, Deppenmeier U (2005) Complete genome sequence of the acetic acid bacterium *Gluconobacter oxydans*. *Nat Biotechnol* 23(2):195–200
- Stephen Dahms A (1974) 3-deoxy-D-pentulosonic acid aldolase and its role in a new pathway of D-xylose degradation. *Biochem Biophys Res Co* 60(4):1433–1439

18. Stephens C, Christen B, Fuchs T, Sundaram V, Watanabe K, Jenal U (2007) Genetic analysis of a novel pathway for D-xylose metabolism in *Caulobacter crescentus*. *J Bacteriol* 189(5):2181–2185
19. Sugiyama M, Suzuki S, Tonouchi N, Yokozeki K (2003) Cloning of the xylitol dehydrogenase gene from *Gluconobacter oxydans* and improved production of xylitol from D-arabitol. *Biosci Biotech Bioch* 67(3):584–591
20. Weimberg R (1961) Pentose oxidation by *Pseudomonas fragi*. *J Biol Chem* 236(3):629–635
21. Yang C, Hua Q, Baba T, Mori H, Shimizu K (2003) Analysis of *Escherichia coli* anaerobic metabolism and its regulation mechanisms from the metabolic responses to altered dilution rates and phosphoenolpyruvate carboxykinase knockout. *Biotechnol Bioeng* 84(2):129–144
22. Zhu K, Lu LF, Wei LJ, Wei DZ, Imanka T, Hua Q (2011) Modification and evolution of *Gluconobacter oxydans* for enhanced growth and biotransformation capabilities at low glucose concentration. *Mol Biotechnol* 49(1):56–64